Surface plasmon on topological insulator/dielectric interface enhanced ZnO ultraviolet photoluminescence

Zhi-Min Liao, Bing-Hong Han, Han-Chun Wu, L. V. Yashina, Yuan Yan et al.

Citation: AIP Advances **2**, 022105 (2012); doi: 10.1063/1.3703320
View online: http://dx.doi.org/10.1063/1.3703320
View Table of Contents: http://aipadvances.aip.org/resource/1/AAIDBI/v2/i2
Published by the AIP Publishing LLC.

Surface plasmon on topological insulator/dielectric interface enhanced ZnO ultraviolet photoluminescence

Zhi-Min Liao,[1,a] Bing-Hong Han,[1] Han-Chun Wu,[2] L. V. Yashina,[3] Yuan Yan,[1] Yang-Bo Zhou,[1] Ya-Qing Bie,[1] S. I. Bozhko,[4] K. Fleischer,[2] I. V. Shvets,[2] Qing Zhao,[1] and Da-Peng Yu[1,a]

[1]*State Key Laboratory for Mesoscopic Physics, Department of Physics, Peking University, Beijing 100871, P.R. China*

[2]*CRANN and School of Physics, Trinity College Dublin, Dublin 2, Ireland*

[3]*Department of Chemistry, Moscow State University, Leninskie Gory, 1/3, 119992 Moscow, Russia*

[4]*Institute of Solid State Physics, Russian Academy of Sciences, Chernogolovka 142432, Russia*

(Received 23 December 2011; accepted 6 March 2012; published online 4 April 2012)

It has recently been predicted that the surface plasmons are allowed to exist on the interface between a topological insulator and vacuum. Surface plasmons can be employed to enhance the optical emission from various illuminants. Here, we study the photoluminescence properties of the ZnO/Bi_2Te_3 hybrid structures. Thin flakes of Bi_2Te_3, a typical three-dimensional topological insulator, were prepared on ZnO crystal surface by mechanical exfoliation method. The ultraviolet emission from ZnO was found to be enhanced by the Bi_2Te_3 thin flakes, which was attributed to the surface plasmon – photon coupling at the Bi_2Te_3/ZnO interface. [http://dx.doi.org/10.1063/1.3703320]

Topological Insulators (TIs) with an insulating band gap in bulk and gapless surface states have attracted a lot of attention.[1] As second generation 3D TIs, Bi_2Se_3 and Bi_2Te_3 are of considerable interest since they have a large bulk energy gap ($\sim$ 0.3 eV) and a simple stable surface state protected by time reversal symmetry.[1–4] Their topological surfaces state may generate Majorana Fermions through the superconducting proximity effect, which could be used to build a quantum computer.[3] The presence of the surface states on Bi_2Se_3 and Bi_2Te_3 have been experimentally identified by reducing the bulk conductance via tuning the gate voltage,[5–7] introducing dopants[8,9] or improving the sample preparation methods.[10,11] Raman spectrum and the Aharonov-Bohm effect were also used to explore the properties of surface carriers.[12,13] Recently, spin and charge collective excitation modes on the surface of a topological insulator were theoretically predicted due to the unique topological properties of the TI materials.[14] Due to the coupling between spin and charge excitations resulting from the locking of the spin and momentum, the spin-plasmon mode was shown to be existing on the surface of a topological insulator.[14] The surface plasmons (SPs) localized at the interface between vacuum and a doped TI with bulk carrier density were also theoretically predicted.[15] Therefore, it would be very interesting to experimentally study the surface plasmons on the TI surface. It is well-known that SP resonances can enhance photoluminescence (PL) from semiconductor emitters and has been observed from various ZnO hybrids structures, such as ZnO/metals,[16,17] ZnO/carbon nanotube[18] and ZnO/graphene.[19] Accordingly, the SPs can be indirectly detected by the SPs-enhanced PL. In this work, we report the enhanced ultraviolet PL in a ZnO/TI hybrid structure induced by SP resonances from thin Bi_2Te_3 flakes. To the best of our knowledge, it is the first experimental demonstration that surface plasmons exist at the TI/ZnO

[a]Address correspondence to liaozm@pku.edu.cn, yudp@pku.edu.cn

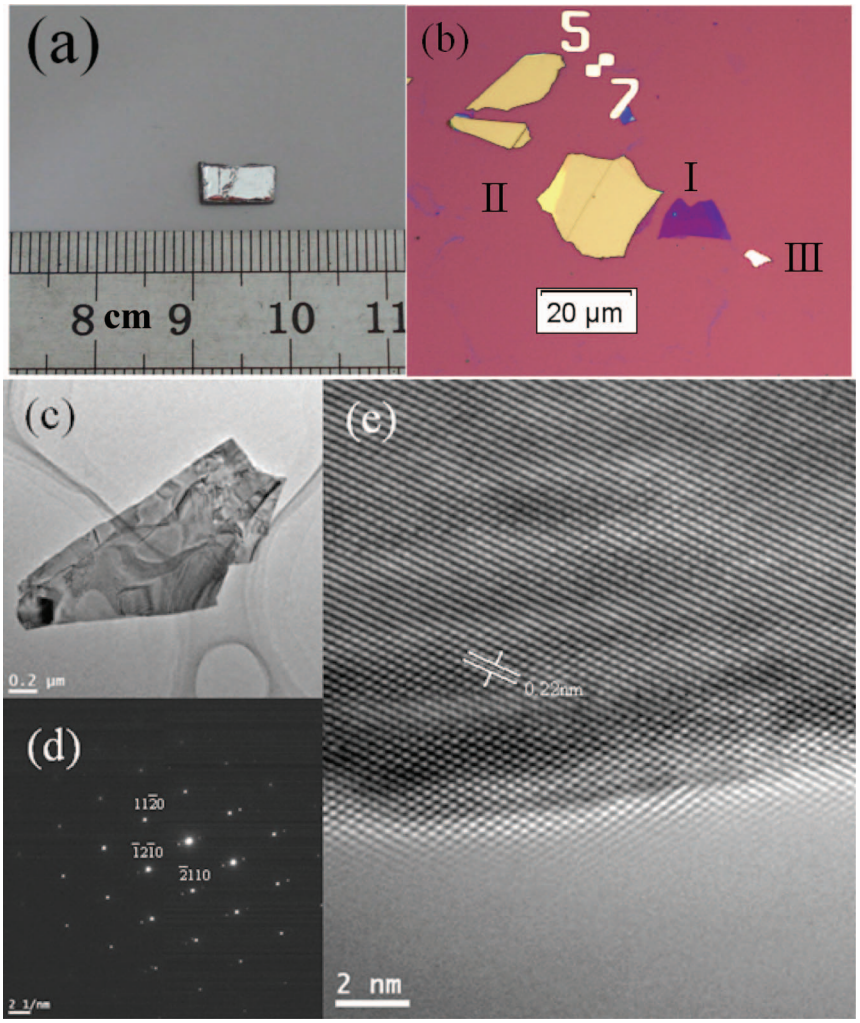

FIG. 1. (a) Bi_2Te_3 sample before exfoliation; (b) Exfoliated Bi_2Te_3 flakes under optical microscope; (c) TEM image of Bi_2Te_3 sample; (d) Selected area electron diffraction (SAED) pattern of Bi_2Te_3 sample; (e) High-resolution TEM image of Bi_2Te_3 sample. The lattice spacing is about 0.22 nm.

interface. Our work has taken an important first step towards verifying the theoretical predications of the surface plasmons induced by the interesting topological properties of the Bi_2Te_3 material.

We used 8×5 mm^2 Bi_2Te_3 piece (Fig. 1(a)) from 100 g crystal. The crystal was obtained by Bridgman method from Te-enriched source using procedure described in.[20] The whole crystal was easily cleaved along growth direction; this is an indication of crystal perfection. Hall measurement showed the n-type of conductivity with bulk carrier concentration of 1×10^{18} cm^{-3} and mobility of about 4500 cm^2/Vs at liquid N_2 temperature.[21] Bi_2Te_3 thin flakes were mechanically exfoliated from the bulk crystal using the scotch-tape method. The thicknesses of the exfoliated samples were estimated under an optical microscope, as shown in Fig. 1(b). Combined with statistics from atomic force microscope (AFM) measurements, our experiments suggest that the purple sample I (marked in the Fig. 1(b)) is less than 100 nm thick, the yellow sample II is about 100∼500 nm thick, while the thickness of the white metal-like sample III is more than 500 nm. To characterize the crystal nature of the microstructures, we transferred the mechanically exfoliated Bi_2Te_3 flakes onto Cu grids for transmission electron microscope (TEM) characterization, as shown in Fig. 1(c). The selected area electron diffraction (SAED) in Fig. 1(d) shows that the sample is single crystal in nature. The high-resolution TEM (HRTEM) image shown in Fig. 1(e) further indicates the mono-crystalline

nature with a lattice spacing of about 0.22 nm, corresponding to the lattice spacing of (11-20) planes of Bi_2Te_3.[5] The scanning electron microscope (SEM) image shown in the Supporting Information Fig. S1(a) clearly indicates the layered character of the Bi_2Te_3 flakes and the exfoliation surface is perpendicular to the c axis with a hexagonal lattice.[22] Fig. S1(b) shows the x-ray energy dispersion spectrum (EDS),[22] suggesting that there are Te vacancies. Thus, a non-zero bulk carrier density is expected.[5,6]

The AFM image in Fig. S2 shows the Bi_2Te_3 flakes on ZnO surface.[22] The thickness of the selected Bi_2Te_3 flake is $\sim$ 140 nm. The PL spectra of the ZnO/Bi_2Te_3 hybrid structures were measured using Renishaw inVia micro PL-Raman systems with an encoded XY-mapping stage. The PL spectra were collected point-by-point along the dashed white line with the direction denoted by the white arrow in the inset of Fig. 2(a). The bottom end of the dashed white line was defined as the reference point (0 μm). PL spectra collected at denoted distance away from the reference point are presented in Fig. 2(a). An enhancement of the PL intensity was unambiguously observed as the collection point approaches the Bi_2Te_3 flake. As shown in Fig. 2(b), a $\sim$ 40% enhancement was observed in the region covered by the Bi_2Te_3 flake. Note, such enhancement does not change the peak position or the shape of the PL spectrum. To further study the PL enhancement of the ZnO/Bi_2Te_3 hybrid structure, two-dimensional mapping of the PL intensity was conducted. The measured Bi_2Te_3 flake on a ZnO crystal is shown in Fig. 3(a). The selected mapping area is denoted by the white rim in the SEM image in Fig. 3(a). The thickness of the Bi_2Te_3 flake is about 150 nm from the AFM measurements (See Fig. S3).[22] The PL intensity mapping was acquired by measuring the PL spectra point-by-point in this area and plotting the peak values of the ultraviolet emission from individual PL spectra. The PL intensity mapping shown in Fig. 3(b) is in accordance with the configuration of the Bi_2Te_3 flake. The PL intensity shows a maximum ($\sim$55% enhancement compared with bare ZnO) in the region covered by the Bi_2Te_3 flake, and gradually decreases as away from the flake.

To rule out any possible laser induced heating effect and show the uniform distribution of the PL intensity from the bare ZnO substrate, we measured the PL spectra in the bare ZnO region left uncovered by Bi_2Te_3 flakes in a linear scanning model with a step size of 10 μm. As shown in Fig. S4, the UV emission from the ZnO substrate is quite uniform with an intensity fluctuation less than 10%.[22]

The coupling between the PL photons from the ZnO and the surface plasmons from the Bi_2Te_3 flake is believed to be responsible for the observed PL enhancement effect. Ordinarily, the PL emission from the ZnO is isotropic and only a small portion of emitted photons will be detected by the measurement system. When a Bi_2Te_3 flake is placed onto the ZnO surface, the emitted photons from the ZnO will be coupled with the SPs on the surface of the Bi_2Te_3 flake and result in a PL enhancement effect. Angle-resolved photoemission spectra studies performed on our crystal indicated a similar Dirac cone structure as in graphene.[21] Therefore, the in-plane wave number dependent energy dispersion relation ω(q) of the SPs for our TI surface can be described in a similar way as done for graphene,[19]

$$\omega(q) = \left[\frac{n_e e^2}{\varepsilon_0(1+\varepsilon_b)m^*}q + \frac{3}{4}v_F^2 q^2\right]^{1/2}, \quad (1)$$

where n_e is the surface carrier density, ε_0 is the vacuum permittivity, ε_b is the background dielectric constant, v_F is the Fermi velocity, and m^* is the effective mass of the electrons. The energy of photons ($\hbar\omega$) in the ultraviolet PL peak of ZnO is 3.3 eV. $\varepsilon_b = 1$ as the sample is surrounded by air. The in-plane momentum $q=2\pi/l$ may be calculated through Eq. (1) utilizing the parameters of n_e, v_F and m^* of Bi_2Te_3. If l is in accordance with the ZnO surface corrugation distance ξ, the strong photon-SP coupling will lead to strong PL enhancement. AFM measurements (Fig. S5) show that ξ of the ZnO crystal is about 3 μm, and the surface-height fluctuation is about 5 nm.[22] SPs scattered by such surface corrugation will be transformed into propagating photons and can be caught again by the detector and thus enhance the measured PL intensity, as shown in Fig. 4(a). The SPs also can reconvert to photons at the Bi_2Te_3 flake edges. We also noticed that the PL enhancement appeared when the PL collection point comes close to but is not on the Bi_2Te_3 flake. In our experiments, the

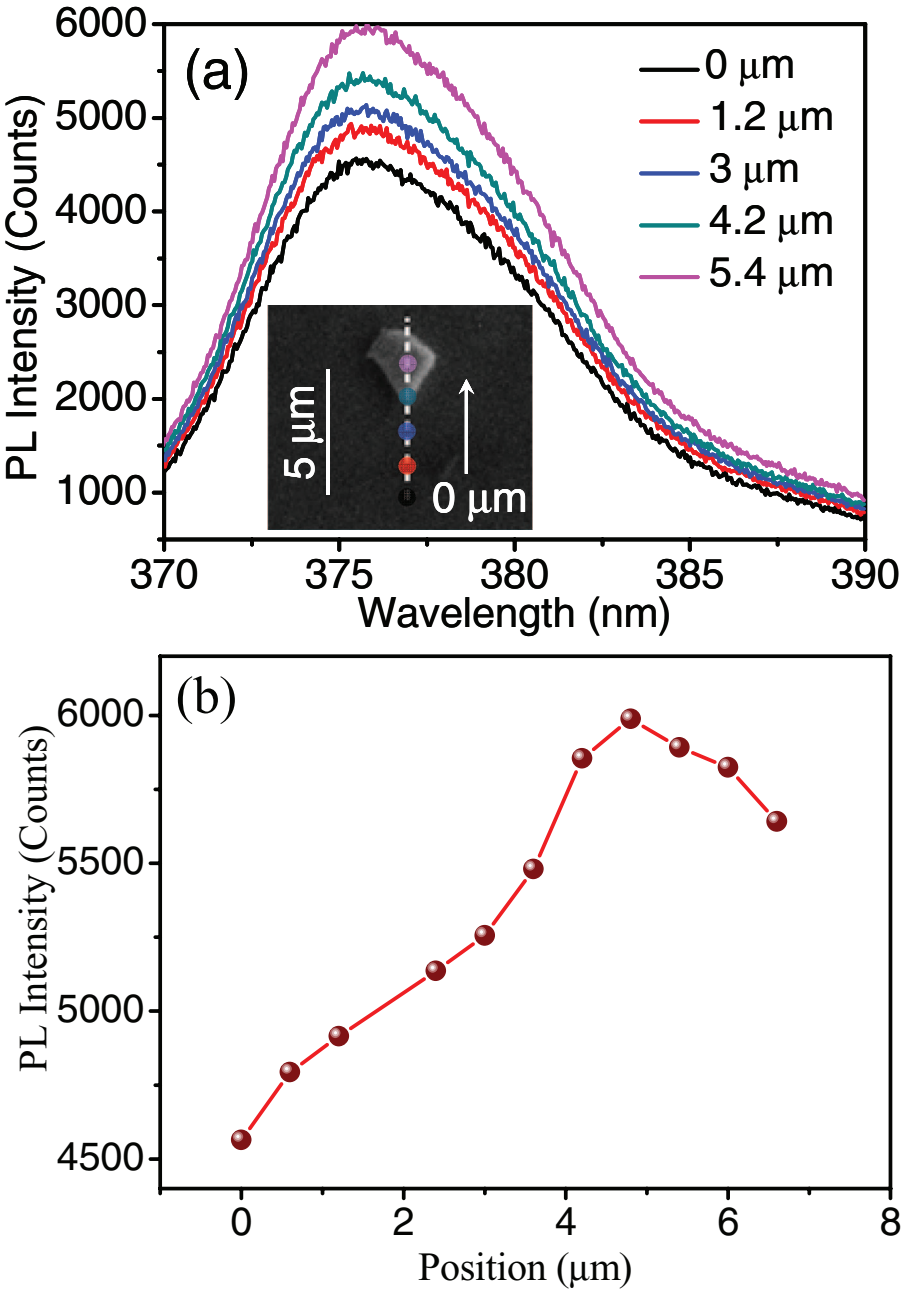

FIG. 2. (a) The PL spectra acquired point-by-point along the white dashed line in the inset. The bottom endpoint of the white dashed line on the inset was defined as starting point (0 μm). Inset: SEM image of the Bi_2Te_3 flake on ZnO surface. (b) The ultraviolet peak intensity vs. distance away from the starting point in the SEM image in (a) Inset.

wavelength of the laser is 325 nm and the diameter of the laser spot is about 1 μm, which is much smaller than the distance between the edge of the Bi_2Te_3 flake and the onset for PL enhancement. The diameter of the laser spot is estimated by illuminating the laser on the polymer and measuring the dimensions of the burned area. Nevertheless, the photons emitted from the ZnO can propagate along the ZnO surface and then couple with the SPs on the Bi_2Te_3 surface, resulting in the PL enhancement, as shown in Fig. 4(b).

There are two main factors that will affect the total PL intensity detected, SPs induced PL enhancement and the optical penetration loss through the Bi_2Te_3. The former depends on the

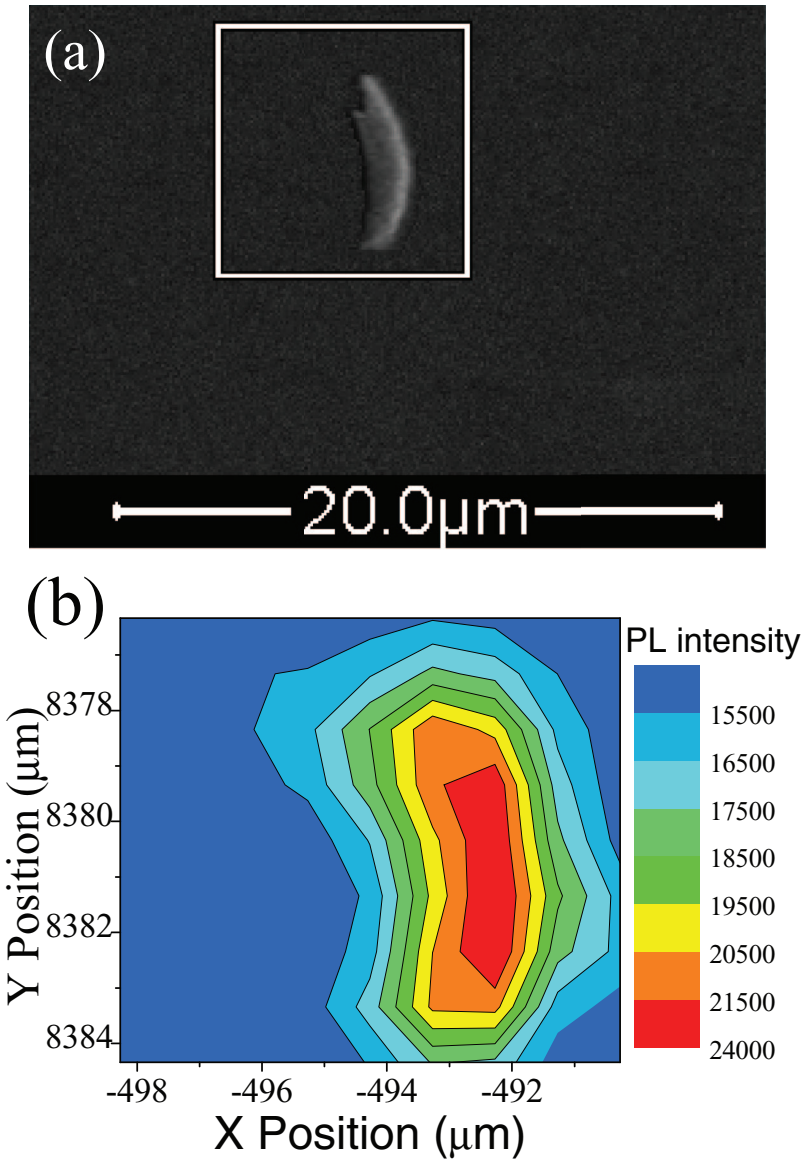

FIG. 3. (a) SEM image of a Bi_2Te_3 flake on ZnO surface and the rectangle with white border indicates the PL scanning area; (b) The 2D distribution of ultraviolet peak intensity corresponds to the rectangle in (a).

intensity of photon-SPs coupling and the relaxation time of SPs, while the later depends on the sample thickness h. To study the optical penetration loss effect, we measured the PL of ZnO covered by Bi_2Te_3 flakes of varying thickness. The experimental results are summarized in Fig. 4(c). Fig. S6 shows the PL intensity in the region covered with a 1.8 μm thick Bi_2Te_3.[22] A reduced PL intensity was observed. The weakening effect may be caused by transmission loss of the incident light on the thicker Bi_2Te_3 sample. To quantitatively describe the weakening effect, we first assume that incident light intensity (I) was attenuated through the Bi_2Te_3 flake with a factor γ, and the intensity exponentially decays with $dI/I = \gamma dh$. Second, the reflection induced optical loss is given by a factor χ. Third, there is a factor α to characterize the photon-SPs coupling induced PL enhancement. Last, the bulk influence (bulk carriers, thermal effect, etc) of the Bi_2Te_3 flake on the PL enhancement is proportional to the thickness (h) with a factor β. Therefore, the PL enhancement Γ (defined as the ratio between the PL intensity on the Bi_2Te_3 flake and on the ZnO substrate) is a function of the

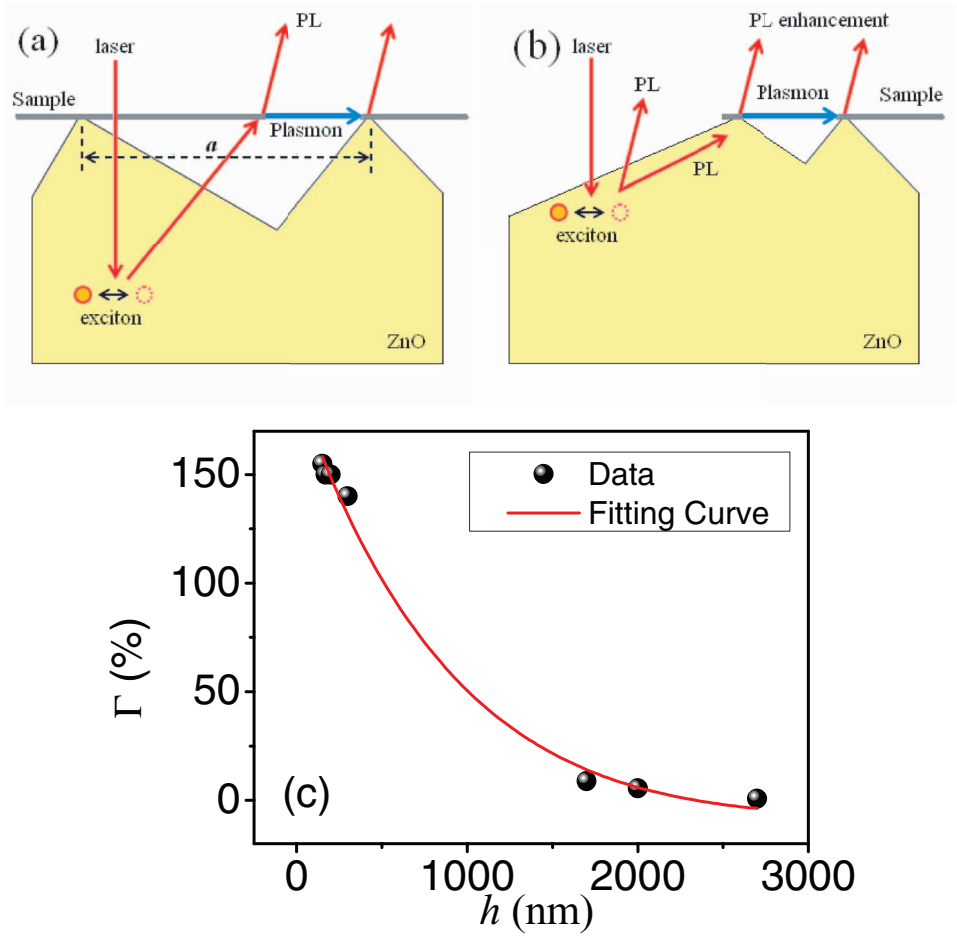

FIG. 4. The scheme of SP induced PL enhancement when (a) laser excitation point is on the Bi_2Te_3 flake and (b) near but not on the Bi_2Te_3 flake. (c) Experimental data and fitting curve of the thickness dependent PL enhancement.

thickness of Bi_2Te_3 flake and can be expressed as

$$\Gamma(h) = (1 - \chi)(\alpha + \beta h)e^{-\gamma h}. \quad (2)$$

The experimental data for the thickness dependent PL enhancement Γ, as shown in Fig. 4(c), can be fitted well by Eq. (2). The parameters can be obtained from the fitting result. $\chi = 0.36 \pm 0.11$ that means the incident laser energy loss from reflection is about 1/3. $\gamma = 0.76 \pm 0.25\ \mu m^{-1}$, suggesting that for micrometer thick samples the optical transmission loss in the PL weakening effect becomes dominant. $\alpha = 2.94 \pm 0.14$, suggesting that the SPs induced PL enhancement is about 3 times of the bare ZnO, similar to the PL enhancement effect of graphene under low temperature.[19] $\beta = -1.26 \pm 0.15\ \mu m^{-1}$, and the negative value means the bulk effect weakens the PL effect. In terms of $(\alpha + \beta h)$, for a thin sample around 200 nm thick $|\beta h| \approx 0.25$, less than 10% of the surface factor α, so the bulk effect can be neglected. The interference of the light inside Bi_2Te_3 thin flakes can also enhance the PL. However, in our experiments, PL enhancement is proportional to the thickness. No oscillation behavior is observed. Therefore, for thin Bi_2Te_3 flakes the PL enhancement effect is mainly a result of contributions from SPs.

In conclusion, we have studied the surface plasmons induced photoluminescence enhancement in ZnO/Bi_2Te_3 hybrid structures. As the thickness of the Bi_2Te_3 flake is less than 200 nm, the detected UV emission from the ZnO region neighboring the Bi_2Te_3 flake was enhanced, but for a micrometer-thick Bi_2Te_3 flake the PL intensity was weakened. The related mechanisms were discussed by considering SP-photon coupling and optical transmission loss.

ACKNOWLEDGMENT

This work was supported by NSFC (No. 10804002), MOST (Nos. 2012CB933401, 2009CB623703), and the Sino Swiss Science and Technology Cooperation Program (2010DFA01810). HCW and IVS acknowledge the financial support from Science Foundation of Ireland (SFI) under Contract No. 06/IN.1/I91.

[1] M. Z. Hasan and C. L. Kane, Rev. Mod. Phys. **82**, 3045 (2010).
[2] H. J. Zhang, C. X. Liu, X. L. Qi, X. Dai, Z. Fang, and S. C. Zhang, Nat. Phys. **5**, 438 (2009).
[3] L. A. Wray, S. Y. Xu, Y. Xia, Y. S. Hor, D. Qian, A. V. Fedorov, H. Lin, A. Bansil, R. J. Cava, and M. Z. Hasan, Nat. Phys. **6**, 855 (2010).
[4] Y. Xia, D. Qian, D. Hsieh, L. Wray, A. Pal, H. Lin, A. Bansil, D. Grauer, Y. S. Hor, R. J. Cava, and M. Z. Hasan, Nat. Phys. **5**, 398 (2009).
[5] D. Kong, W. Dang, J. J. Cha, H. Li, S. Meister, H. Peng, Z. Liu, and Y. Cui, Nano Lett. **10**, 2245 (2010).
[6] J. Chen, H. J. Qin, F. Yang, J. Liu, T. Guan, F. M. Qu, G. H. Zhang, J. R. Shi, X. C. Xie, C. L. Yang, K. H. Wu, Y. Q. Li, and L. Lu, Phys. Rev. Lett. **105**, 176602 (2010).
[7] H. Steinberg, D. R. Gardner, Y. S. Lee, and P. Jarillo-Herrero, Nano Lett. **10**, 5032 (2010).
[8] J. G. Checkelsky, Y. S. Hor, R. J. Cava, and N. P. Ong, Phys. Rev. Lett. **106**, 196801 (2011).
[9] A. Saji, S. Ampili, S. Yang, K. J. Ku, and M. Elizabeth, J. Phys.: Condens. Matter. **17**, 2873 (2005).
[10] H. Tang, D. Liang, R. L. J. Qiu, and X. P. A. Gao, ACS Nano **5**, 7510 (2011).
[11] M. Z. Hossain, S. L. Rumyantsev, K. M. F. Shahil, D. Teweldebrhan, M. Shur, and A. A. Balandin, ACS Nano **5**, 2657 (2011).
[12] S. Y. F. Zhao, C. Beekman, L. J. Sandilands, J. E. J. Bashucky, D. Kwok, N. Lee, A. D. LaForge, S. W. Cheong, and K. S. Burch, Appl. Phys. Lett. **98**, 141911 (2010).
[13] H. Peng, K. Lai, D. Kong, S. Meister, Y. Chen, X. L. Qi, S. C. Zhang, Z. X. Shen, and Y. Cui, Nat. Mater. **9**, 225 (2010).
[14] S. Raghu, S. B. Chung, X.-L. Qi, and S.-C. Zhang, Phys. Rev. Lett. **104**, 116401 (2010).
[15] A. Karch, Phys. Rev. B **83**, 245432 (2011).
[16] D. Y. Lei, J. Li, and H. C. Ong, Appl. Phys. Lett. **91**, 021112 (2007).
[17] J. Li and H. C. Ong, Appl. Phys. Lett. **92**, 121107 (2007).
[18] S. Kim, D. H. Shin, C. O. Kim, S. W. Hwang, S.-H. Choi, S. Ji, and J.-Y. Koo, Appl. Phys. Lett. **94**, 213113 (2009).
[19] S. W. Hwang, D. H. Shin, C. O. Kim, S. H. Hong, M. C. Kim, J. Kim, K. Y. Lim, S. Kim, S.-H. Choi, K. J. Ahn, G. Kim, S. H. Sim, and B. H. Hong, Phys. Rev. Lett. **105**, 127403 (2010).
[20] V. I. Shtanov and L. V. Yashina, J. Cryst. Growth **311**, 3257 (2009).
[21] M. R. Scholz, D. Marchenko, A. Varykhalov, A. Volykhov, L. V. Yashina, and O. Rader, arXiv:1108.1053v1 (to be published).
[22] See supplementary material at http://dx.doi.org/10.1063/1.3703320 for the SEM images and AFM images of the thick Bi_2Te_3 flakes and their corresponding effects on the ZnO ultraviolet emissions.